

## Effects of Microstructure on Fatigue Crack Propagation and Crack Closure Behavior in Aluminum Alloy 7150

E. ZAIKEN\* and R. O. RITCHIE

Department of Materials Science and Mineral Engineering, University of California, Berkeley, CA 94720 (U.S.A.)

(Received June 8, 1984; in revised form August 20, 1984)

### ABSTRACT

*A study has been made of the role of aging treatment in influencing fatigue crack propagation and crack closure behavior in a high purity ingot metallurgy aluminum alloy 7150, with specific reference to crack growth at low and high load ratios in the near-threshold regime. A trend of increasing growth rates and decreasing threshold stress intensity  $\Delta K_{th}$  values with increased aging was seen to be consistent with lower measured levels of crack closure and a decreasing tortuosity in crack path. On the basis of crack growth measurements in moist room air, where closure due to corrosion product formation was found to be negligible in this alloy, the superior fatigue resistance of underaged microstructures (compared with overaged structures of similar strength and peak-aged structures of higher strength) was attributed to greater slip reversibility and to enhanced roughness-induced crack closure and deflection from the more tortuous crack paths. Such factors are promoted in alloy systems hardened by coherent shearable precipitates where the mode of deformation is one of non-homogeneous planar slip.*

### 1. INTRODUCTION

Recent studies into the mechanics and mechanisms of fatigue have identified a prominent role of crack closure in influencing crack propagation behavior (see for example refs. 1-26). This is particularly apparent at low growth rates (*i.e.* below about  $10^{-6}$  mm cycle<sup>-1</sup>) near the fatigue threshold stress intensity range  $\Delta K_{th}$  for no crack growth. In

this regime the origin of such closure has been associated with mechanisms such as crack surface corrosion deposits [3-6], irregular fracture morphologies coupled with crack tip shear displacements [7-9] and fluid-induced pressure [12], in addition to conventional mechanisms relying on cyclic plasticity [1] (Fig. 1). The effect of the closure, which induces contact between mating fracture surfaces at positive stress intensities  $K_{cl}$  during the loading cycle, is to reduce the local driving force for crack advance from nominally applied levels, *e.g.*  $\Delta K = K_{max} - K_{min}$ , to some near-tip effective level  $\Delta K_{eff} = K_{max} - K_{cl}$  [1] where  $K_{max}$ ,  $K_{min}$ ,  $K_{cl}$  and  $\Delta K$  are the maximum stress intensity, minimum stress intensity, closure stress intensity and range of stress intensities respectively.

On the basis mainly of data in steels, the effects of variable-amplitude loading, frequency, load ratio, microstructure, environment and temperature have all been associated with closure phenomena (for a review see ref. 26). In non-ferrous alloys, however, less information exists. Elber [1] and Schmidt and Paris [2] first applied the concept of (plasticity-induced) closure to cyclic behavior in aluminum alloys in an attempt to explain variable-amplitude loading and load ratio effects in these alloys. Subsequent studies in this system have focused largely on effects of microstructure and environment [13-22]. Petit and Zeghoul [13] and Vasudévan and Suresh [14] identified a role of oxide-induced closure, although enhanced crack surface oxide films were only detected in overaged aluminum alloy 7075 and, unlike behavior in steels [4-6], were not consistent with lower growth rates. The more important mechanism in aluminum alloys appears to be associated with roughness-induced closure, where it has been suggested that the strongly crystal-

\*Present address: Shiley Incorporated, Irvine, CA 92714, U.S.A.

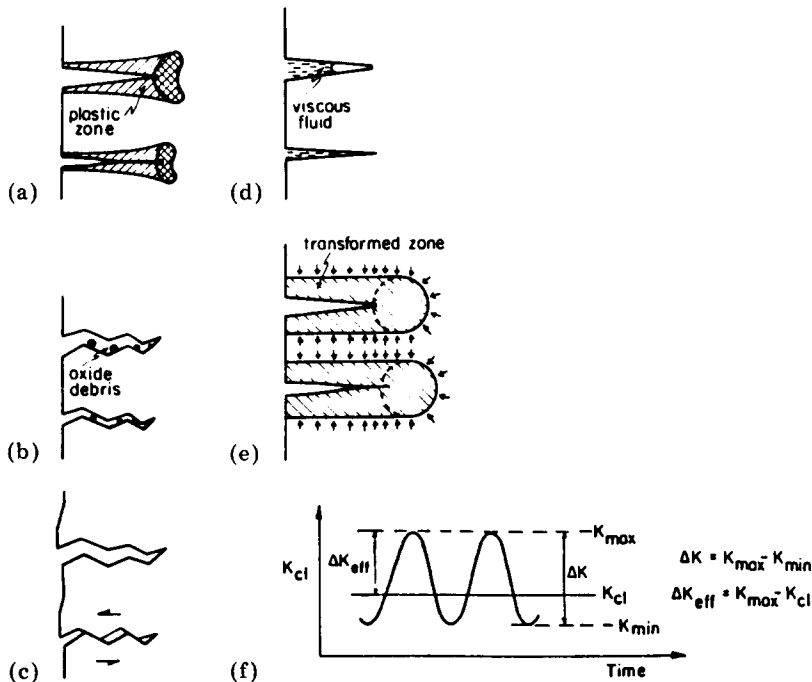


Fig. 1. (a)-(e) Schematic illustration of the primary mechanisms of fatigue crack closure ((a) plasticity-induced closure; (b) oxide-induced closure; (c) roughness-induced closure; (d) viscous-fluid-induced closure; (e) phase-transformation-induced closure) and (f) the nomenclature required in the definition of stress intensities representative of the fatigue cycle.

lographic nature of crack paths [27-32], particularly in underaged structures, promotes closure [17-20] and crack deflection [19, 20, 33] and thus reduces near-threshold growth rates. Recently, these concepts of deflection and closure have been applied to rationalize the microstructural effects on fatigue crack growth in aluminum alloy 7075 [19]. The decreasing threshold stress intensity  $\Delta K_{th}$  values with increasing aging treatment were attributed to a smaller influence of closure associated with less crystallographic crack paths although, apart from oxide thickness measurements, detailed crack closure measurements were not made.

In the present work, effects of microstructure during precipitation hardening are examined on fatigue crack propagation in a high purity aluminum alloy 7150 in the light of quantitative measurements of oxide film thickness, fracture surface roughness and closure stress intensity values. It is shown that near-threshold growth rates are slowest in underaged structures, consistent with the highest measured closure loads, and the most deflected crack paths. No evidence of oxide-induced closure could be detected.

## 2. EXPERIMENTAL PROCEDURES

Conventionally cast ingot metallurgy aluminum alloy 7150 was supplied by Alcoa with the composition shown in Table 1. The Al-Zn-Mg-Cu alloy, which is a high purity version of aluminum alloy 7050 (with lower silicon and iron contents), was received as plate 25 mm thick in the solution-treated and 2% stretched (W51) condition. Samples for fatigue and tensile testing were machined at quarter-thickness and three-quarters-thickness locations and tempered to produce underaged, peak-aged (T6) and overaged (T7) structures. The specific heat treatments and resulting room temperature uniaxial tensile properties are shown in Tables 2 and 3 respectively. The underaged and overaged heat treatments were designed to produce structures with approximately similar yield strength. Transmission electron micrographs of the three microstructures are shown in Fig. 2. Underaged structures are characterized by coherent Guinier-Preston zones roughly 4-8 nm in diameter, which on further aging are replaced by semicoherent intermetallic  $\eta'$  precipitates ( $MgZn_2$ - $Mg(CuAl)_2$ ) in the peak-

TABLE 1

Nominal chemical composition

| Element                                | Si   | Fe   | Cu   | Mg   | Zn   | Ti   | Zr   | Al      |
|--|------|------|------|------|------|------|------|---------|
| Amount (wt.%) of element in alloy 7150 | 0.07 | 0.11 | 2.10 | 2.16 | 6.16 | 0.02 | 0.13 | Balance |

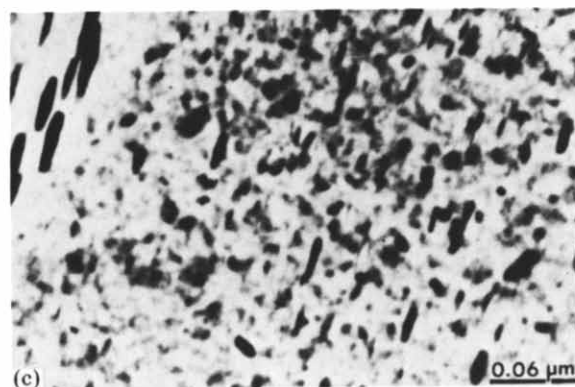
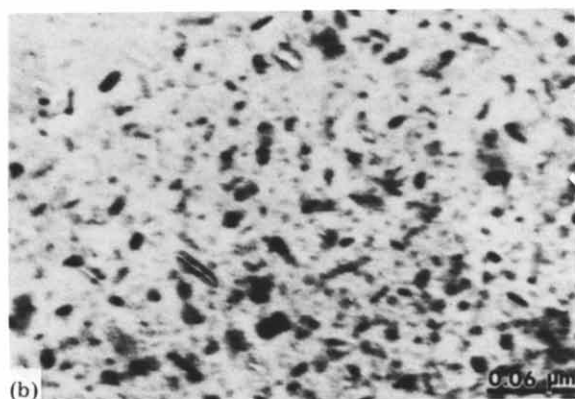
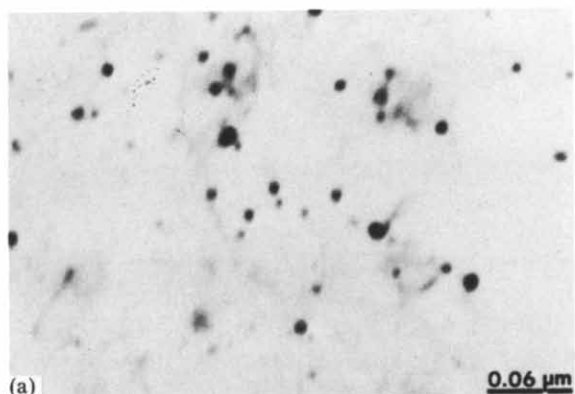


Fig. 2. Transmission electron micrographs of (a) underaged, (b) peak-aged (T6) and (c) overaged (T7) ingot metallurgy aluminum alloy 7150.

aged condition. In overaged structures, predominately incoherent  $\eta$  phase precipitates ( $\text{MgZn}_2$  compounds) are found in both the matrix and the grain boundaries (with small

TABLE 2

Heat treatments utilized for tests on alloy 7150

| Condition      | Heat treatment                                    |
|----------------|---|
| Underaged      | ST <sup>a</sup> + 1½ h at 121 °C                  |
| Peak aged (T6) | ST <sup>a</sup> + 100 h at 121 °C                 |
| Overaged (T7)  | ST <sup>a</sup> + 24 h at 121 °C + 40 h at 163 °C |

<sup>a</sup>ST, solution treated, quenched and stretched 2% (W51 condition).

precipitate-free zones of half-width about 30 nm), together with coarsened  $\eta'$  in the matrix. There is also evidence of small dispersoid particles (e.g.  $\text{Al}_3\text{Zr}$ ) of less than 10 nm in diameter. Grains were somewhat elongated along the rolling direction with an approximate size of 15  $\mu\text{m}$  by 5  $\mu\text{m}$ .

Fatigue crack growth tests were performed in controlled room temperature air (22 °C; relative humidity, 45%) on compact tension test pieces 6.4 mm thick machined in the TL orientation (*i.e.* the load was applied in the long transverse direction and the crack propagated in the longitudinal direction). Using d.c. electrical potential techniques to monitor crack growth, tests were performed under load control at 50 Hz (sine wave) frequency with load ratios  $R (= K_{\min}/K_{\max})$  of 0.10 and 0.75. Near-threshold crack propagation rates were determined under manual load-shedding (decreasing  $\Delta K$ ) conditions and checked under increasing  $\Delta K$  conditions. The threshold level  $\Delta K_{\text{th}}$  was defined as the highest  $\Delta K$  level giving growth rates less than  $10^{-8}$  mm cycle<sup>-1</sup> [34], with the majority of tests duplicated.

Macroscopic crack closure measurements to determine  $K_{\text{cl}}$  values were performed *in situ* with the back-face strain technique using two strain gauges to record strain both parallel and perpendicular to the loading axis (Fig. 3) [22, 24]. Mean closure loads were deduced from the point during the loading cycle where the resulting elastic compliance curves of load *versus* relative strain deviated from linearity. Crack surface corrosion deposits were mea-

TABLE 3

Room temperature mechanical properties of alloy 7150

| Condition      | Yield strength (MPa) | Ultimate tensile strength (MPa) | Elongation <sup>a</sup> (%) | Reduction in area (%) | Work-hardening exponent |
|----------------|----------------------|---------------------------------|-----------------------------|-----------------------|-------------------------|
| Underaged      | 371                  | 485                             | 6.8                         | 12.1                  | 0.055                   |
| Peak aged (T6) | 404                  | 480                             | 6.0                         | 10.3                  | 0.046                   |
| Overaged (T7)  | 372                  | 478                             | 7.1                         | 12.5                  | 0.058                   |

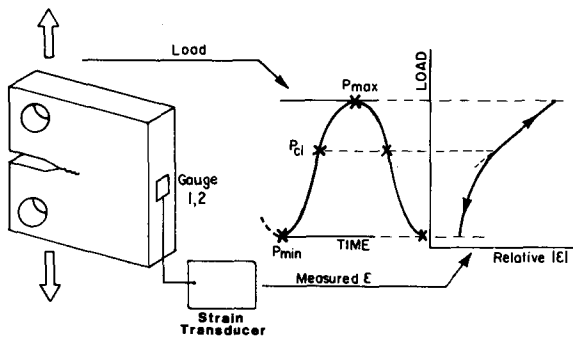
<sup>a</sup>On a 32 mm gauge length.

Fig. 3. Schematic illustration of the back-face strain technique used to estimate closure stress intensity  $K_{cl}$  values.  $P_{max}$ ,  $P_{min}$  and  $P_{cl}$  are the maximum, minimum and closure loads respectively.

sured by scanning Auger spectroscopy using an  $Ar^+$  sputter rate of  $45 \text{ \AA min}^{-1}$  [25]. The excess oxide thickness, representing the excess material inside the crack, was computed with a Pilling-Bedworth ratio of 1.3 for  $Al_2O_3$ , assuming oxide growth in only the thickness direction and equal thicknesses on each face. The degree of fracture surface roughness was assessed from scanning electron and optical micrographs of the crack paths in terms of the ratio of total length of the crack to the projected length on the plane of maximum tensile stress.

### 3. RESULTS

#### 3.1. Growth rate behavior

The variation in fatigue crack propagation rates  $da/dN$  with stress intensity range  $\Delta K$  for alloy 7150 in the underaged, peak-aged and overaged conditions is shown in Fig. 4 for load ratios of 0.10 and 0.75. Although growth rates above about  $10^{-6} \text{ mm cycle}^{-1}$  are similar at each load ratio for all three microstruc-

tures, at near-threshold levels it is evident that underaged structures show the highest fatigue resistance in terms of lowest growth rates and highest threshold  $\Delta K_{th}$  values. Similar behavior has been reported for other aluminum alloys, including ingot metallurgy 7075 [15-19], 7475 [20, 31] and powder metallurgy 7091 [32]. Compared with those for the underaged structure, the threshold  $\Delta K_{th}$  values in the present results are roughly 15% and 28% lower in the peak-aged and overaged structures respectively at  $R = 0.10$  (Table 4). Thresholds are similarly reduced with increased aging at  $R = 0.75$ , although the absolute magnitude of the differences in  $\Delta K_{th}$  values is much smaller.

#### 3.2. Crack closure data

Corresponding crack closure data, in terms of back-face strain measurements of  $K_{cl}/K_{max}$  as a function of  $\Delta K$ , are shown in Fig. 5 for the three microstructures at both  $R = 0.10$  and  $R = 0.75$ . Similar to behavior reported for several ferrous and non-ferrous alloys at low load ratios (see for example refs. 20-24), the degree of crack closure at  $R = 0.10$  increases sharply with decreasing  $\Delta K$  level, approaching a maximum of  $K_{cl}/K_{max}$  close to unity at  $\Delta K_{th}$ . Although no evidence of closure could be detected experimentally in any microstructure at  $R = 0.75$ , at low load ratios the underaged structures showed the highest closure levels, consistent with their highest thresholds.

#### 3.3. Fractography

Scanning electron micrographs of the fatigue fracture surfaces close to  $\Delta K_{th}$  in the three aging conditions are shown in Fig. 6. The fractography is transgranular in all cases with evidence of slip steps, ledges and facets. Such facets are particularly pronounced in

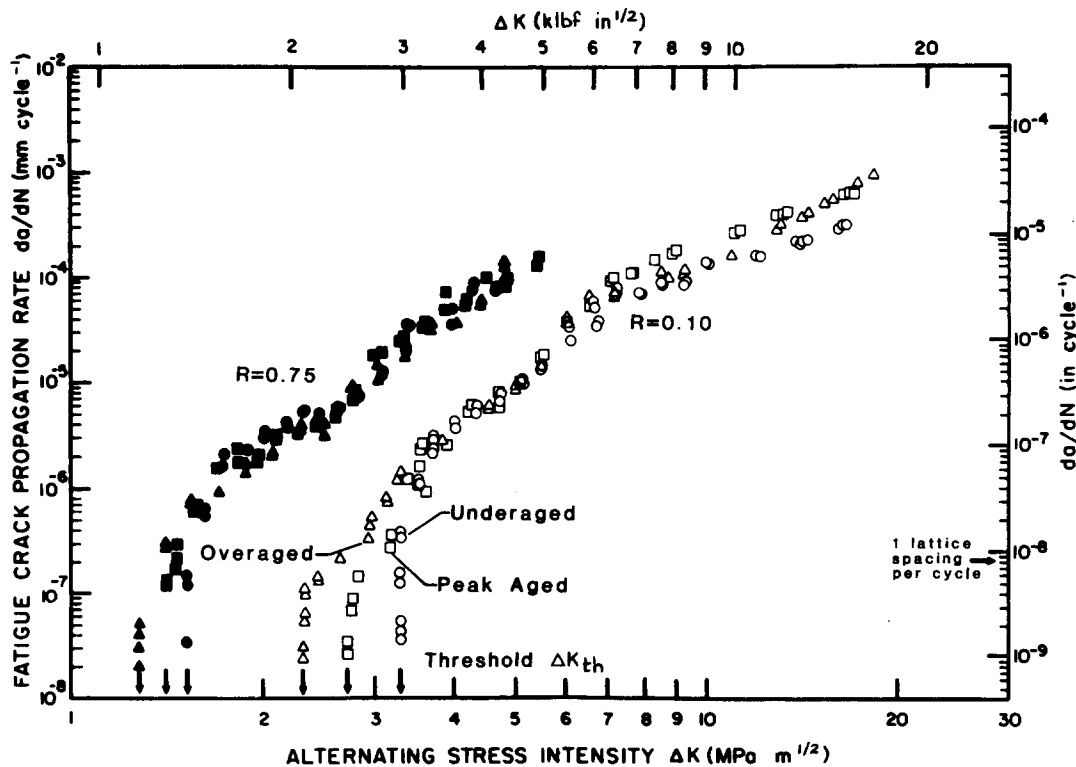


Fig. 4. Variation in fatigue crack growth rate  $da/dN$  as a function of stress intensity range  $\Delta K$  for ingot metallurgy aluminum alloy 7150 tested at  $R = 0.10$  and  $R = 0.75$  in controlled moist air. Data are shown for underaged, peak-aged (T6) and overaged (T7) microstructures.

| Condition | Symbol for the following load ratios |            |
|-----------|--------------------------------------|------------|
|           | $R = 0.1$                            | $R = 0.75$ |
| Underaged | ○                                    | ●          |
| Peak aged | □                                    | ■          |
| Overaged  | △                                    | ▲          |

TABLE 4

Threshold data for alloy 7150 at load ratios of 0.10 and 0.75

| Condition      | Load ratio<br>$K_{min}/K_{max}$ | $\Delta K_{th}$<br>(MPa m <sup>1/2</sup> ) | $\Delta CTOD^a$<br>(nm) | Maximum<br>$K_{cl}/K_{th}^a$ | Excess oxide<br>thickness <sup>a</sup><br>(nm) | Degree of<br>roughness <sup>b</sup> |
|----------------|---------------------------------|--|-------------------------|------------------------------|--|-------------------------------------|
| Underaged      | 0.10                            | 3.05-3.31                                  | 100                     | 0.88                         | ≈ 3  | 1.26                                |
|                | 0.75                            | 1.51                                       | 22                      | 0                            | ≈ 3  |                                     |
| Peak aged (T6) | 0.10                            | 2.44-2.94                                  | 65                      | 0.85                         | ≈ 3  | 1.21                                |
|                | 0.75                            | 1.27                                       | 14                      | 0                            | ≈ 3  |                                     |
| Overaged (T7)  | 0.10                            | 2.23-2.33                                  | 50                      | 0.77                         | ≈ 3  | 1.06                                |
|                | 0.75                            | 1.16                                       | 13                      | 0                            | ≈ 3  |                                     |

<sup>a</sup>At the threshold  $\Delta K_{th}$ .

<sup>b</sup>The ratio of the total crack length to the projected length on the plane of maximum tensile stress.

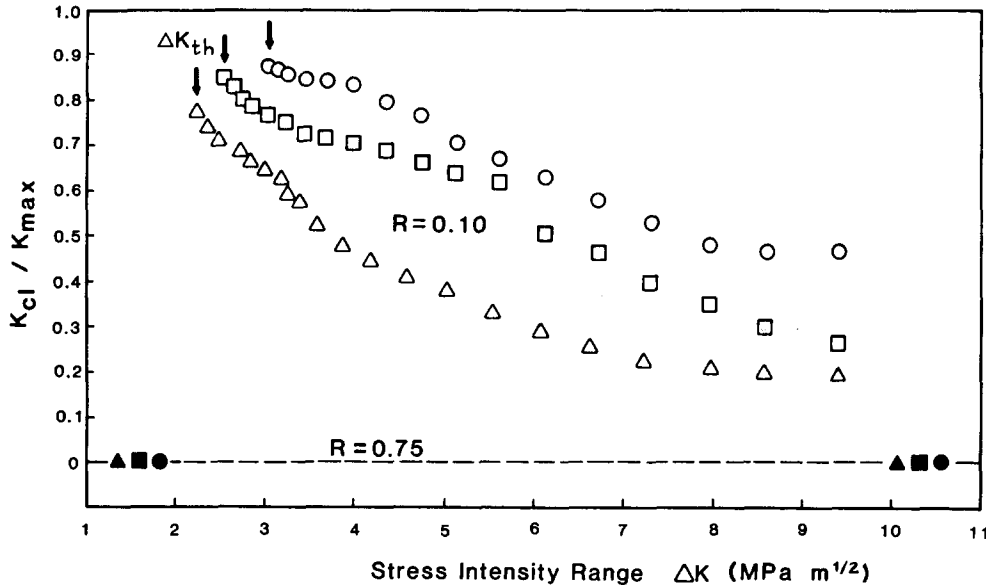


Fig. 5. Variation in crack closure, in terms of the ratio  $K_{cl}/K_{max}$  of closure stress intensity to maximum stress intensity, as a function of  $\Delta K$  for underaged ( $\circ$ ,  $\bullet$ ), peak-aged (T6) ( $\square$ ,  $\blacksquare$ ) and overaged (T7) ( $\triangle$ ,  $\blacktriangle$ ) alloy 7150 at  $R = 0.10$  and  $R = 0.75$ .

the underaged structure and have an appearance characteristic of crystallographic fatigue surfaces [27, 35, 36]. The rougher or more tortuous nature of the crack path in the underaged structures can be seen more clearly in Fig. 7 where crack profiles are shown for the three conditions. In contrast with the zig-zag appearance of underaged fractures, crack paths in the overaged structures are predominantly linear with far fewer crack deflections.

Associated Auger measurements of the extent of crack surface corrosion deposits are shown in Fig. 8. In marked contrast with behavior in lower strength steels [6, 25], there is no evidence in this present alloy of any pronounced oxide accumulation within the crack even at threshold levels. Oxide films were similar for all aging conditions at both load ratios with a measured thickness of the order of 3 nm, comparable with the limiting thickness of naturally occurring oxides in this alloy. Such results are similar to those reported for alloy 7075 in the underaged and peak-aged conditions. However, they are in contrast with those reported for overaged alloy 7075, where excess oxide thicknesses approached 100 nm at  $\Delta K_{th}$  ( $R = 0.33$ ) [14]. As listed in Table 4, the excess oxide film thicknesses in alloy 7150 are small compared with computed values of the cyclic crack-tip-

opening displacements  $\Delta CTOD$ , indicating that, for this alloy tested in room air environments, the contribution from oxide-induced crack closure is likely to be minimal.

#### 4. DISCUSSION

Similar to other aluminum alloys [17-20, 27-33], the present results on a high purity ingot metallurgy alloy 7150 indicate clearly that underaged microstructures have superior near-threshold fatigue crack propagation resistance to overaged and peak-aged microstructures. This is seen in terms of lower growth rates below about  $10^{-6}$  mm cycle $^{-1}$  and higher threshold  $\Delta K_{th}$  values at both low and high load ratios, although the magnitude of the effect is diminished at  $R = 0.75$  (Fig. 4). The higher thresholds in the underaged structures are consistent with increased crack closure (Fig. 5), faceted and crystallographic fracture surfaces (Fig. 6) and more tortuous crack paths (Fig. 7), compared with the smoother more linear (undeflected) crack morphology in overaged structures. Data indicating this trend of lower thresholds with decreasing  $K_{cl}/K_{max}$  values and decreasing degrees of fracture surface roughness for increasing aging are listed in Table 4.

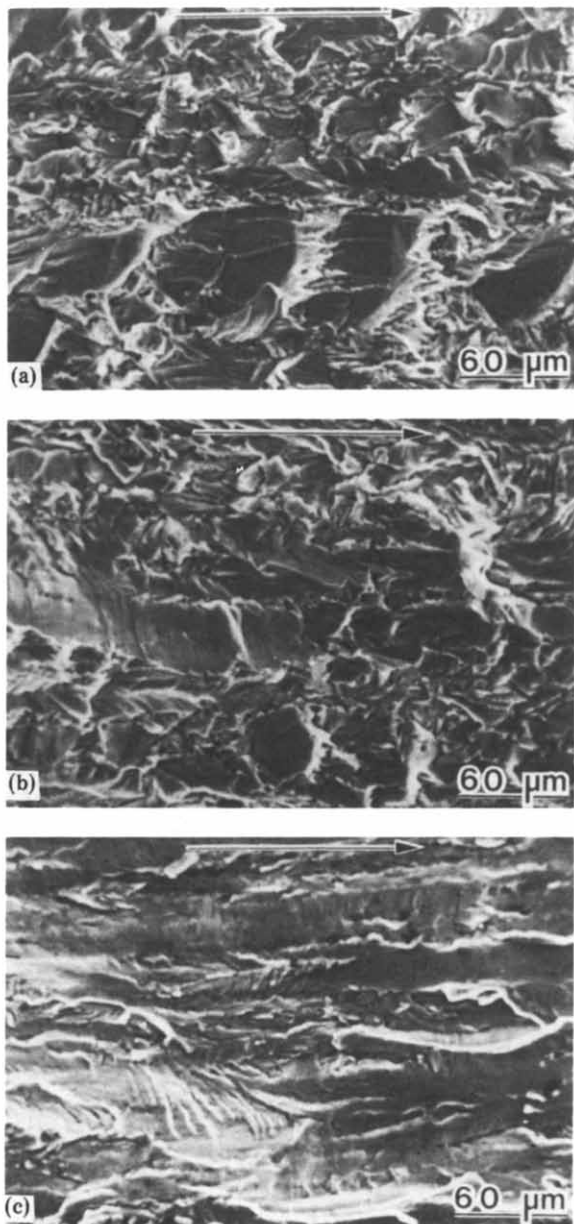


Fig. 6. Scanning electron micrographs of fatigue fracture surfaces close to  $\Delta K_{th}$  ( $R = 0.10$ ) in ingot metallurgy aluminum alloy 7150, showing the morphology in (a) underaged, (b) peak-aged (T6) and (c) overaged (T7) microstructures. Horizontal arrows indicate direction of crack growth.

In keeping with current notions on the role of crack closure [26], this trend (which has been similarly rationalized in alloys 7075 [17, 19] and 7475 [20]) is to be expected. Akin to behavior in dual-phase steels [23, 24],  $\beta$  annealed titanium [37, 38] and Al-Li alloys [39], the generation of a meandering crack path (either by crack deflection at harder

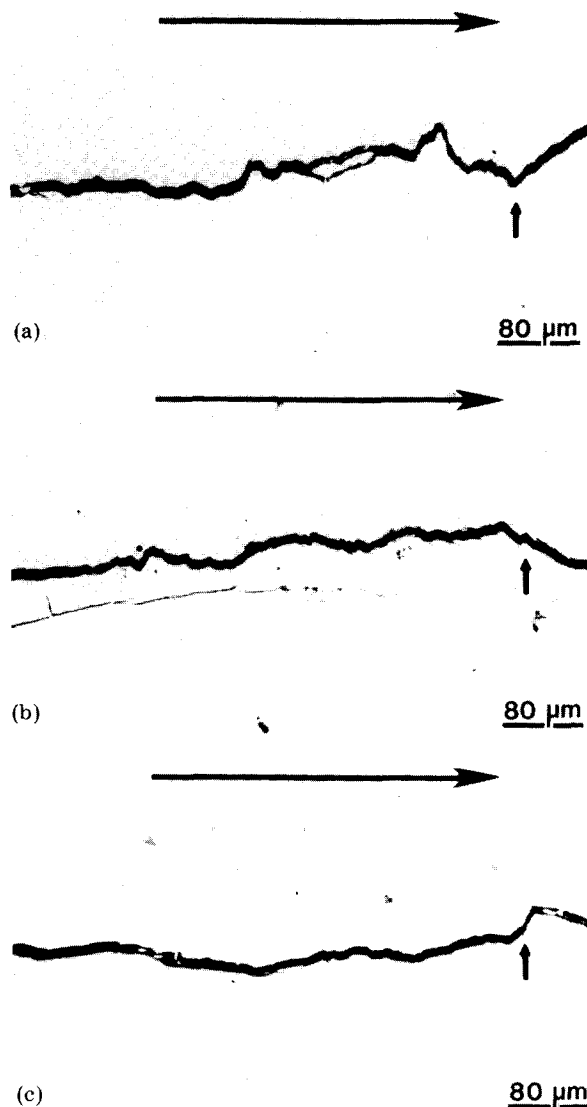


Fig. 7. Crack path morphology of near-threshold fatigue cracks in ingot metallurgy aluminum alloy 7150 in the (a) underaged, (b) peak-aged (T6) and (c) overaged (T7) conditions. Horizontal arrows indicate direction of crack growth; vertical arrows indicate the location of crack arrest at  $\Delta K_{th}$ .

phases [23, 24, 33] or in the present case by crystallographic deflection at grain boundaries) can lead to slower fatigue crack growth rates through a reduction in local crack driving force. This results from three major factors: (i) a lower effective  $da/dN$  due to a longer path length of the crack, (ii) lower effective stress intensities at the crack tip due to crack deflection from the plane of maximum tensile stress [33] and (iii) lower effective ranges of stress intensities at the crack tip due to the resulting production of increased crack

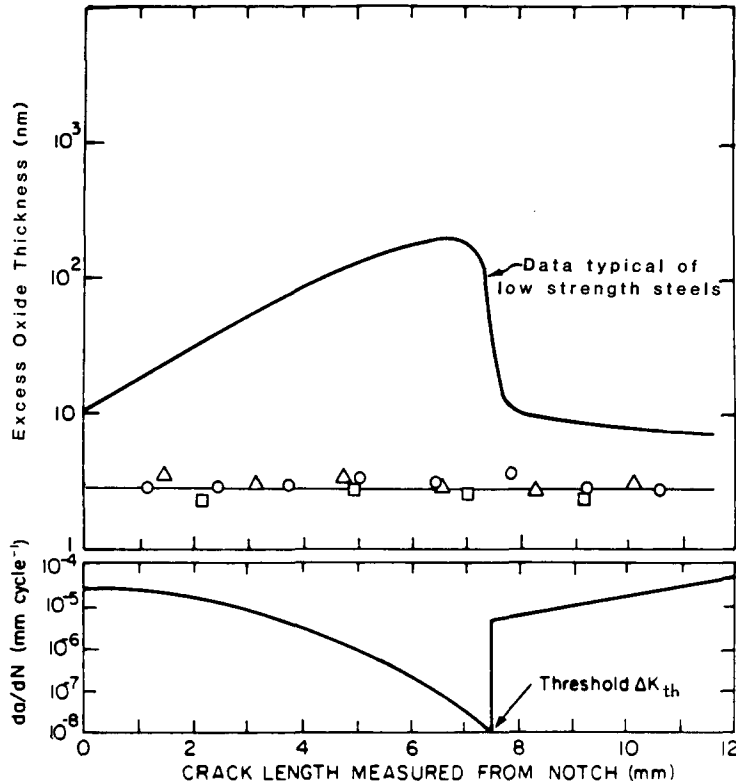


Fig. 8. Scanning Auger spectroscopy measurements of excess crack surface oxide deposits as a function of fatigue crack length and growth rate  $da/dN$ . Data points for ingot metallurgy aluminum alloy 7150 in the underaged, peak-aged and overaged microstructures ( $R = 0.10$ ) are compared with prior data [6] on lower strength steels at low load ratios.

closure from asperity contact behind the crack tip [7-9]. Since the thicknesses of crack surface oxide films are so small compared with  $\Delta CTOD$  values, it appears that the major contribution to this closure in the present alloy originates from the roughness-induced mechanism (Fig. 1) aided by the rough out-of-plane crack morphologies and the crack tip shear displacements [40] which result. These effects are far less pronounced in the overaged structures where crack paths are more linear (Fig. 7) such that corresponding crack growth rates are higher. Furthermore, at the high load ratios, differences between underaged and overaged microstructures are reduced because the role of crack closure is diminished at the larger crack-opening displacements (Fig. 5).

This argument is consistent with previous explanations based solely on microstructural factors [28]. In underaged precipitation-hardening systems, where the mode of alloy hardening is primarily the shearing of small coherent precipitates, the resulting hetero-

geneous deformation (*i.e.* coarse planar slip) promotes a crystallographic crack path. Because slip is occurring on fewer slip systems, the degree of slip reversibility is greater and hence the crack tip damage per cycle is less. Conversely, in overaged systems where the mode of hardening is now Orowan bypassing of semicoherent or incoherent larger non-shearable precipitates, the resulting homogeneous deformation (*i.e.* wavy slip) generates a far more planar fracture surface because of the larger number of finer slip steps. This leads to greater slip irreversibility and more crack tip damage per cycle. Furthermore, as noted by Zedalis *et al.* [31], the larger precipitate-free zones in overaged 7000 series aluminum alloys arising from the growth of incoherent grain boundary precipitates must contribute somewhat to the lower fatigue resistance in these microstructures.

Finally, it is interesting to note that the microstructures which show superior fatigue crack growth resistance at near-threshold

levels do not necessarily retain such resistance at higher growth rates [41, 42]. For example, although the effect is not apparent in alloy 7150 (Fig. 4), underaged microstructures in many aluminum alloys show faster growth rates above about  $10^{-6}$  mm cycle<sup>-1</sup> and slower growth rates close to  $\Delta K_{th}$ , compared with overaged structures. Such observations tend to support explanations based on crack closure since at higher growth rates, with associated larger crack-tip-opening displacements, the effect of closure mechanisms relying on asperity contact (*i.e.* roughness-induced mechanisms) would be reduced. Conversely, where crack closure and deflection mechanisms are important (*e.g.* for transient crack growth behavior under variable-amplitude loading conditions), underaged structures clearly show the longest post-overload retardations and the highest general resistance to crack growth [42]. However, these planar slip characteristics of coherent particle precipitation-hardened systems, which are so important in generating superior-fatigue crack growth resistance through inhomogeneous deformation, rough crystallographic crack paths and enhanced closure and deflection, can lead simultaneously to inferior crack initiation toughness from a greater tendency for strain localization. This is particularly evident in Al-Li alloys where the increased coherency between lithium-containing intermetallics and the matrix can result in exceptionally good fatigue crack propagation resistance [43] through enhanced crack path tortuosity [39] and yet at the same time can produce extremely low fracture toughness values [44].

## 5. CONCLUSIONS

Based on a study of fatigue crack propagation behavior in high purity ingot metallurgy aluminum alloy 7150 tested at high and low load ratios in moist air with underaged, peak-aged and overaged microstructures, the following conclusions can be made.

(i) With increased aging, resistance to fatigue crack extension is decreased, in the form of faster near-threshold growth rates and lower fatigue threshold  $\Delta K_{th}$  values, consistent with reduced measured levels of crack closure and a decreasing tortuosity in crack path.

(ii) The superior fatigue crack growth resistance of the underaged structures is attributed to greater slip reversibility and to enhanced roughness-induced crack closure and deflection from more tortuous crack paths, factors which result from the non-homogeneous planar slip characteristics of deformation in microstructures hardened by coherent (shearable) precipitates.

(iii) Crack flank corrosion deposits in all microstructures were small compared with near-threshold crack-tip-opening displacements at both load ratios, indicating that the contribution from oxide-induced crack closure in this alloy is minimal.

## ACKNOWLEDGMENTS

This work was funded by the U.S. Air Force Office of Scientific Research under Grant AFOSR 82-0181. The authors are also grateful to Alcoa for provision of the alloy and to the Alcoa Foundation for additional support.

Thanks are also due to Drs. A. H. Rosenstein, S. Suresh and W. Yu for helpful discussions and to Patsy Donehoo and Darrel Frear for experimental assistance.

## REFERENCES

- 1 W. Elber, *Damage Tolerance in Aircraft Structures*, ASTM Spec. Tech. Publ. 486, 1981, p. 230.
- 2 R. A. Schmidt and P. C. Paris, *Progress in Flaw Growth and Fracture Toughness Testing*, ASTM Spec. Tech. Publ. 536, 1973, p. 79.
- 3 P. C. Paris, R. J. Bucci, E. T. Wessel, W. G. Clark and T. R. Mager, *Stress Analysis and Growth of Cracks*, Proc. Natl. Symp. on Fracture Mechanics, 1981, in ASTM Spec. Tech. Publ. 513, 1972, p. 141.
- 4 R. O. Ritchie, S. Suresh and C. M. Moss, *J. Eng. Mater. Technol.*, 102 (1980) 293.
- 5 A. T. Stewart, *Eng. Fract. Mech.*, 13 (1980) 463.
- 6 S. Suresh, G. F. Zamiski and R. O. Ritchie, *Metall. Trans. A*, 12 (1981) 1435.
- 7 N. Walker and C. J. Beevers, *Fatigue Eng. Mater. Struct.*, 1 (1979) 135.
- 8 K. Minakawa and A. J. McEvily, *Scr. Metall.*, 15 (1981) 937.
- 9 S. Suresh and R. O. Ritchie, *Metall. Trans. A*, 13 (1982) 1627.
- 10 P. K. Liaw, T. R. Leax, R. S. Williams and M. G. Peck, *Metall. Trans. A*, 13 (1982) 1607.
- 11 W. W. Gerberich, W. Yu and K. Esaklul, *Metall. Trans. A*, 15 (1984) 875.

- 12 J.-L. Tzou, S. Suresh and R. O. Ritchie, *Acta Metall.*, 32 (1984), in the press.
- 13 J. Petit and A. Zeghoul, in J. Bäcklund, A. Blom and C. J. Beevers (eds.), *Proc. 1st Int. Conf. on Fatigue Thresholds, Stockholm, June 1-3, 1981*, Vol. 1, Engineering Materials Advisory Services, Warley, 1982, p. 563.
- 14 A. K. Vasudévan and S. Suresh, *Metall. Trans. A*, 13 (1982) 2271.
- 15 K. Schulte, H. Nowack and K. H. Trautmann, *Z. Werkstofftech.*, 11 (1980) 287.
- 16 J. Petit, P. Renaud and P. Violan, *Proc. 14th Eur. Conf. on Fracture, Leoben, 1982*, Engineering Materials Advisory Services, Warley, 1982, p. 426.
- 17 M. C. Lafarie-Frenot and C. Gasc, *Fatigue Eng. Mater. Struct.*, 6 (1983) 329.
- 18 J. Petit, in D. L. Davidson and S. Suresh (eds.), *Proc. Int. Symp. on Fatigue Crack Growth Threshold Concepts*, Metallurgical Society of AIME, Warrendale, PA, 1984, p. 3.
- 19 S. Suresh, A. K. Vasudévan and P. E. Bretz, *Metall. Trans. A*, 15 (1984) 369.
- 20 R. D. Carter, E. W. Lee, E. A. Starke and C. J. Beevers, *Metall. Trans. A*, 15 (1984) 555.
- 21 R. J. Asaro, L. Hermann and J. M. Baik, *Metall. Trans. A*, 12 (1981) 1133.
- 22 E. Zaiken and R. O. Ritchie, *Scr. Metall.*, 18 (1984) 847.
- 23 K. Minakawa, Y. Matsuo and A. J. McEvily, *Metall. Trans. A*, 13 (1982) 439.
- 24 V. B. Dutta, S. Suresh and R. O. Ritchie, *Metall. Trans. A*, 15 (1984) 1193.
- 25 S. Suresh, D. M. Parks and R. O. Ritchie, in J. Bäcklund, A. Blom and C. J. Beevers (eds.), *Proc. 1st Int. Conf. on Fatigue Thresholds, Stockholm, June 1-3, 1981*, Vol. 1, Engineering Materials Advisory Services, Warley, 1982, p. 391.
- 26 S. Suresh and R. O. Ritchie, in D. L. Davidson and S. Suresh (eds.), *Proc. Int. Symp. on Fatigue Crack Growth Threshold Concepts*, Metallurgical Society of AIME, Warrendale, PA, 1984, p. 227.
- 27 G. G. Garrett and J. F. Knott, *Acta Metall.*, 23 (1975) 841.
- 28 E. Hornbogen and K. H. Zum Gahr, *Acta Metall.*, 24 (1976) 581.
- 29 J. Lindgkeit, A. Gysler and G. Lütjering, *Metall. Trans. A*, 12 (1981) 1613.
- 30 F. S. Lin and E. A. Starke, in I. M. Bernstein and A. W. Thompson (eds.), *Proc. Int. Conf. on Hydrogen Effects in Metals, Moran, 1980*, Metallurgical Society of AIME, Warrendale, PA, 1981, p. 485.
- 31 M. Zedalis, L. Filler and M. E. Fine, *Scr. Metall.*, 16 (1982) 471.
- 32 M. Zedalis and M. E. Fine, *Scr. Metall.*, 16 (1982) 1411.
- 33 S. Suresh, *Metall. Trans. A*, 14 (1983) 2375.
- 34 R. O. Ritchie, *Int. Metall. Rev.*, 20 (1979) 205.
- 35 M. Gell and G. R. Leverant, *Acta Metall.*, 16 (1968) 553.
- 36 J. F. McCarver and R. O. Ritchie, *Mater. Sci. Eng.*, 55 (1982) 63.
- 37 G. R. Yoder, L. A. Cooley and T. W. Crooker, *Metall. Trans. A*, 8 (1977) 1737.
- 38 G. R. Yoder, L. A. Cooley and T. W. Crooker, *Metall. Trans. A*, 9 (1978) 1413.
- 39 A. K. Vasudévan, P. E. Bretz, A. C. Miller and S. Suresh, *Mater. Sci. Eng.*, 64 (1984) 113.
- 40 D. L. Davidson, *Fatigue Eng. Mater. Struct.*, 3 (1981) 229.
- 41 R. J. Bucci, A. B. Thakker, T. H. Saunders, R. R. Sawtell and J. T. Staley, in D. F. Bryan and J. M. Potter (eds.), *Effect of Load Variables on Fatigue Crack Initiation and Propagation, ASTM Spec. Tech. Publ. 714*, 1980, p. 41.
- 42 S. Suresh and A. K. Vasudévan, in D. L. Davidson and S. Suresh (eds.), *Proc. Int. Symp. on Fatigue Crack Growth Threshold Concepts*, Metallurgical Society of AIME, Warrendale, PA, 1984, p. 361.
- 43 E. J. Coyne, T. H. Sanders, Jr., and E. A. Starke, Jr., in T. H. Sanders, Jr., and E. A. Starke, Jr. (eds.), *Proc. 1st Int. Conf. on Aluminium-Lithium Alloys, Stone Mountain, GA, 1981*, Metallurgical Society of AIME, Warrendale, PA, 1981, p. 293.
- 44 E. S. Balmuth and R. Schmidt, in T. H. Sanders, Jr., and E. A. Starke, Jr. (eds.), *Proc. 1st Int. Conf. on Aluminium-Lithium Alloys, Stone Mountain, GA, 1981*, Metallurgical Society of AIME, Warrendale, PA, 1981, p. 69.